Evolution of the Snow Area Index of the Subarctic Snowpack in Central Alaska over a Whole Season. Consequences for the Air to Snow Transfer of Pollutants

A.-S. TAILLANDIER,[†,‡] F. DOMINE,[*,†,‡] W. R. SIMPSON,[‡,§] M. STURM,[||] T. A. DOUGLAS,[||] AND K. SEVERIN[⊥]

CNRS, Laboratoire de Glaciologie et Géophysique de l'Environnement, BP 96, 38402 Saint-Martin d'Hères Cedex, France, Geophysical Institute, Department of Chemistry, and Department of Geology and Geophysics, University of Alaska Fairbanks, Fairbanks, Alaska 99775, and U.S. Army Cold Regions Research and Engineering Laboratory, Fort Wainwright, Alaska 99703

The detailed physical characteristics of the subarctic snowpack must be known to quantify the exchange of adsorbed pollutants between the atmosphere and the snow cover. For the first time, the combined evolutions of specific surface area (SSA), snow stratigraphy, temperature, and density were monitored throughout winter in central Alaska. We define the snow area index (SAI) as the vertically integrated surface area of snow crystals, and this variable is used to quantify pollutants' adsorption. Intense metamorphism generated by strong temperature gradients formed a thick depth hoar layer with low SSA (90 $cm^2\ g^{-1}$) and density (200 $kg\ m^{-3}$), resulting in a low SAI. After snowpack buildup in autumn, the winter SAI remained around 1000 m^2/m^2 of ground, much lower than the SAI of the Arctic snowpack, 2500 $m^2\ m^{-2}$. With the example of PCBs 28 and 180, we calculate that the subarctic snowpack is a smaller reservoir of adsorbed pollutants than the Arctic snowpack and less efficiently transfers adsorbed pollutants from the atmosphere to ecosystems. The difference is greater for the more volatile PCB 28. With climate change, snowpack structure will be modified, and the snowpack's ability to transfer adsorbed pollutants from the atmosphere to ecosystems may be reduced, especially for the more volatile pollutants.

Introduction

Snow is a material with a high surface area (*1*) that interacts with atmospheric chemistry through processes such as adsorption of trace gases, trapping of particles, and catalysis of heterogeneous photochemical reactions, resulting in a major impact on polar atmospheric chemistry (*2*). For example, measurements and models showed that falling snow adsorbs semivolatile organic chemicals (SVOCs) and removes them from the troposphere more efficiently than rain (*3*, *4*). Once deposited, the seasonal snow cover represents an active reservoir for trace gases that is supplied by precipitation and dry deposition events. The snowpack may subsequently release these trace gases to the atmosphere (*5*−*8*) through processes involved in metamorphism, such as those that reduce snow surface area available for gas adsorption (*9*, *10*). Alternatively, these gases may be transferred to terrestrial and marine ecosystems during snowmelt, supplying both nutrients and toxic contaminants with adverse effects on all life forms (*11*). Understanding air−snow exchanges of trace gases is therefore important to understand atmospheric chemistry and the air−ecosystems exchange of chemicals in polar regions and also to be able to reconstruct past atmospheric compositions from ice cores (*12*, *13*).

To quantify air/snow exchanges of adsorbed species, one needs to know the specific surface area (SSA) of snow, i.e., its surface area accessible to gases (*14*), usually expressed in $cm^2\ g^{-1}$. Houdier et al. (*8*) observed a fairly good correlation ($R^2 = 0.70$) between acetaldehyde concentrations in Arctic snow and snow SSA, from which they deduced that adsorption onto snow crystal surfaces was one of several mechanisms explaining the incorporation of CH_3CHO into the snowpack. Herbert et al. (*15*) observed a rapid decrease of SVOCs concentrations in snow associated with the aging of surface layers. They proposed that this re-emission of contaminants to the atmosphere was due to the decrease in snow SSA, although that variable was not measured.

To date, only a few studies have measured the SSA of the snowpack. The only investigation of the potential of the whole snowpack for the adsorption of trace gases is that of Dominé et al. (*1*), who measured what they called the total surface area (TSA) of the Arctic snow cover, once in February and once in April. The definition of the TSA is the vertically integrated surface area of snow, expressed in m^2/m^2 of ground. This dimensionless variable is calculated from the sum for all snow layers of the product of SSA ($cm^2\ g^{-1}$), density ($g\ cm^{-3}$), and thickness (cm) of each layer. Here, by analogy to the leaf area index (LAI) used to characterize surface exchanges between the vegetation and the atmosphere (*16*), we propose to rename this variable "snow area index" (SAI). Dominé et al. (*1*) observed an increase in Arctic snowpack SAI from 1720 $m^2\ m^{-2}$ in winter to 2740 $m^2\ m^{-2}$ in spring, corresponding to the increase in snow accumulation. In subarctic environments, the snowpack shows different characteristics and has been called the taiga snowpack by Sturm et al. (*17*). Together with the Arctic snowpack [also known as "tundra" snowpack (*17*)], both represent the most important types of snow cover on Earth, with regard to spatial and temporal extent. Yet there is no data about the SAI of the subarctic snowpack.

This paper describes for the first time the evolution of the subarctic snowpack SAI during an entire winter to quantify its potential for gas uptake from and release to the atmosphere. Snowpack stratigraphy, temperature, and density profiles were also monitored. The crystal morphological changes associated with snow metamorphism were followed using optical and environmental scanning electron microscopes (ESEM). An application to chemical aspects is given as an example of the impact of the subarctic snow cover on atmospheric composition. This work complements that of Sturm and Benson (*18*), who produced a detailed study of

* Corresponding author e-mail: florent@lgge.obs.ujf-grenoble.fr.
† CNRS.
‡ Geophysical Institute, University of Alaska Fairbanks.
§ Department of Chemistry, University of Alaska Fairbanks.
|| U.S. Army Cold Regions Research and Engineering Laboratory.
⊥ Department of Geology and Geophysics, University of Alaska Fairbanks.

10.1021/es060842j CCC: $33.50
Published on Web 11/15/2006

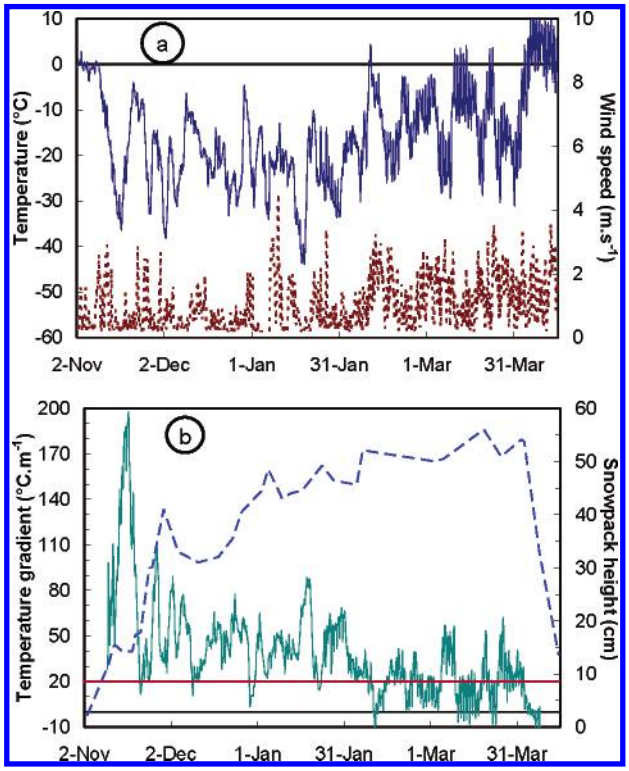

FIGURE 1. (a) Air temperature and wind speed (dotted line), respectively at 60 cm and 3 m above the ground surface during the winter 2003/2004 at the LARS site, central Alaska. (b) Mean temperature gradient in the snowpack and snowpack height (dashed line). The temperature gradient is calculated between the snow/ground interface and the buried sensor closest to the top of the snowpack. The critical temperature gradient of 20 C m^{-1} thought to be necessary for depth hoar development (*21, 22*) is marked by a horizontal line.

the seasonal evolution of the subarctic snowpack but did not measure SSA or SAI.

Methods

Field Measurements. The seasonal subarctic snowpack was studied during winter 2003/2004 at the Large Animal Research Station (LARS) of the University of Alaska Fairbanks (64°52′ N/147°44′ W). The snowpack was sampled at least weekly or more frequently as dictated by snowfalls. The sampling procedure is described in earlier work (*1*, *19*). Briefly, a new snow pit with vertical faces was dug each time to observe the stratigraphy and identify the layers of interest. Density was measured continuously with an accuracy of about 5% by weighing a core of known volume. A 3-cm resolution was used at the top of the snowpack and 5-cm resolution deeper down, regardless of layer boundaries, as some layers were too thin to be measured individually. For SSA measurement, about 100 cm^3 of snow was collected in a glass vial with a stainless steel spatula thermally equilibrated with the snow. The vial was immediately immersed in liquid nitrogen to stop metamorphism until its content was transferred to the SSA measurement container in a cold room at −17 °C. Each snow sample was observed and photomicrographs were taken under reflected light with a reflex camera fitted with bellows and a macrolens. Additional images were obtained with an ESEM, as detailed earlier (*20*).

To measure the temperature gradient in the snowpack, a vertical string of temperature sensors with 7.5-cm spacing connected to a data logger was positioned on the study field before the first snowfall. Meteorological data continuously monitored on site included air temperature and wind speed, respectively 0.6 and 3 m above the ground (Figure 1a).

Measurements of the Specific Surface Area of Snow. Snow SSA was measured by adsorption of methane at liquid nitrogen temperature (77 K), as detailed in Legagneux et al. (*14*). A mathematical treatment (*23*) was applied to the adsorption isotherm obtained to derive the SSA. The method has a reproducibility of 6% and an accuracy better than 12% (*14*). In comparison to the work of Legagneux et al. (*14*), the shape of the stainless steel container holding the snow sample and of the tubing connecting it to the pump were modified to reduce pumpdown time and to facilitate snow transfer into the container. The volume of the container holding the snow was reduced to half its previous value in this new configuration.

After the release of Legagneux et al. (*14*), an experimental artifact due to CH_4 adsorption on the stainless steel walls of the container holding the snow was detected, as already mentioned by Legagneux et al. (*14*) and detailed in Domine et al. (*25*). Its effects were quantified by measuring the adsorption isotherm of CH_4 on the empty container and corrected by considering simultaneously both adsorption equilibria on stainless steel and snow. The magnitude of the correction increased with decreasing surface area of the sample. It was less than 10% for samples with a surface area greater than 1 m^2 (this applies to >90% of samples) and increased to 50% below 0.2 m^2.

Results

Meteorology. Central Alaska is marked by a cold continental climate with dry winters. Mean annual precipitations is 270 mm with a summer maximum, the driest month being April (http://climate.gi.alaska.edu). The study site was chosen for its open forest conditions. Central Alaska is not very windy, resulting in frequent strong temperature inversions. Over the winter, wind speed did not exceed 4.5 m s^{-1} (16 km h^{-1}) at 3 m height (Figure 1). Wind speed was somewhat higher at the end of winter. Snow accumulation was low: the snowpack reached its maximum height of 55 cm by mid-March (Figure 1), but most of the accumulation took place in November−December. This was a typical winter season, as the mean maximum height over the last 60 years is 57 ± 20 cm (http://climate.gi.alaska.edu). The snowpack formed from precipitation events a few centimeters thick at the most. The snow cover lasted over 5 months, from the end of October to mid-April. The onset of snowpack buildup was a bit late, as it usually starts in early October. Air temperature averaged −15 °C throughout this time period (Figure 1a), with a mean of −23 °C in December−January. Once snow first deposited, the snow/ground interface remained frozen, with an average temperature of −3.6 °C between November 10 and April 1 with a minimum of −5.7 °C on February 1. The cold air temperature together with a thin snowpack allowed the establishment of strong temperature gradients, reaching a maximum of 198 °C m^{-1} when the snowpack was only 15 cm deep in November (Figure 1b).

Snowpack Morphology and Stratigraphy. The study site was in a fairly planar and gently south sloping open field. Falling snow was not intercepted by the canopy, providing a homogeneous snow cover at the 100 m scale, enabling a good reproducibility between contiguous snow pits. This kind of open forest landscape is reasonably representative of Fairbanks surroundings, and the observed stratigraphy corresponds well to what Sturm et al. (*17*) called a taiga snowpack, with the stratigraphic sequence close to that described in Sturm and Benson (*18*). In forested areas, however, snow accumulation and SAI are smaller, because up to 40% of precipitation is lost to interception by the canopy and subsequent sublimation (*26*). Other causes of spatial variations include wind that transports snow (*27*), but this is not a strong actor in the taiga, and synoptic variations in weather (*27*). From trips within a 150 km radius around

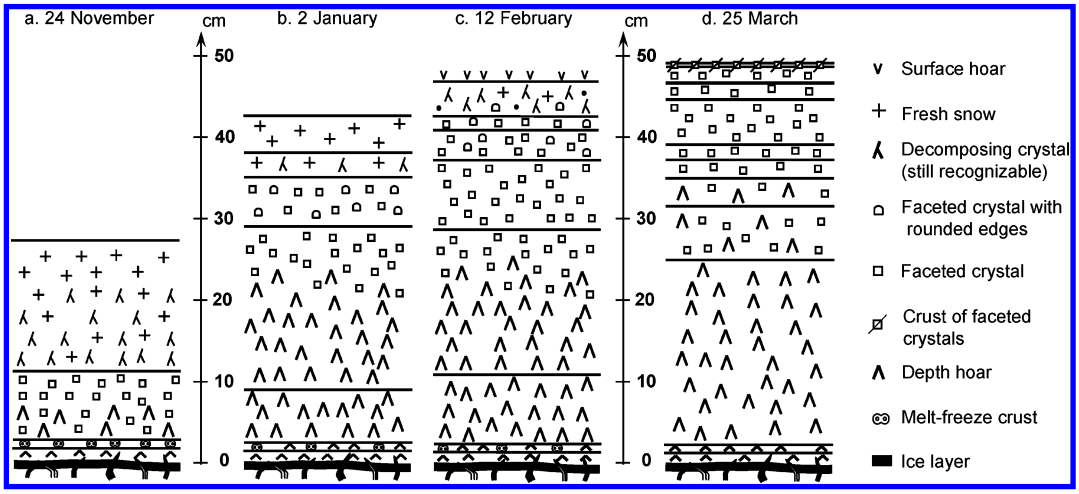

FIGURE 2. Stratigraphy of the natural snowpack on the ground at four different stages in winter 2003/2004.

Fairbanks, we estimate that about 90% of snowpack heights were within 50% of the value at our site that year, i.e., 27 to 82 cm, with a similar snowpack structure. To a first approximation, we suggest that this 50% factor also applies to SAI.

The evolution of crystal morphology was observed throughout the winter in a layer near the base of the snowpack, fallen on November 10. Photomicrographs of snow crystals at various stages of evolution are shown in the Supporting Information. In contrast to isothermal metamorphism, where crystal shapes remain recognizable after weeks or even months (*28*), here the strong temperature gradient generates large water vapor fluxes that accelerate metamorphism. Changes in grain shapes are readily observable after a few hours. Facets grow and initial crystal shapes are not recognizable after a couple of days. Crystals then become striated and after about two weeks fully transform into faceted hollow crystals of depth hoar. They subsequently kept growing under the continuous water vapor flux. In late March, many depth hoar crystals exceeded 10 mm in their longest dimension.

This temporal evolution is also seen in a vertical section of the snowpack: recognizable precipitated crystals at the top, turning to faceted crystals a few centimeters down, and finally fully developed depth hoar crystals in the bottom part of the pack. Figure 2 represents four stages in the evolution of the snowpack during winter 2003/2004. In the stratigraphies presented, what distinguishes a layer from another is an abrupt change in at least one aspect between the strata above and below [as defined in ICSSG (*29*)]. There is no layer limit when the grain transition is continuous and delicate to locate precisely.

Following the first snowfalls of the season, rain, freezing rain, and snow falls alternated for a week in late October/early November. This formed a basal ice layer 1−2 cm thick that was covered by a 1.5 cm thick snow layer, above which a hard melt/freeze crust 1 cm thick formed. The basal ice layer looked fairly airtight in early winter, preventing most of the vapor flux from the ground from penetrating the snowpack [see picture exemplifying a basal ice layer; class 8bi in ICSSG (*29*)]. The uppermost crust consisted of submillimetric rounded refrozen crystals and was still permeable. In January, however, metamorphism led to the growth of depth hoar crystals within the crust itself. With ongoing metamorphism, depth hoar crystals in the lower part of the snowpack (between 2.5 and 11 cm in height) developed to form noncohesive vertical "chains of grains" (*21*, *30*), while still increasing in size, up to 10 mm in February. The upper part of the snowpack also kept metamorphosing, with faceting of newly precipitated layers. Limits between layers became less and less visible with metamorphism and depth. As spring approached, daily thermal cycling increased, enhancing transient temperature gradients in the top few centimeters of the snowpack. This accelerated the metamorphism of new snow, relative to the early part of winter.

At the end of winter, a continuous 25-cm layer of depth hoar was visible at the base of the snowpack (Figure 2d). Crystal sizes increased from 3 to 4 mm at the top of this layer, to up to 15 mm under the former melt/freeze crust, now transformed into hard depth hoar. The thick basal ice had also metamorphosed with depth hoar crystals growing on its upper side. A mild wind event also formed a thin fragile wind crust in late March (Figure 2d).

Specific Surface Area of Snow Layers. Density and SSA profiles at the four stages described in Figure 2 are shown in Figure 3. Fresh snow density ranged from 20 to 90 kg m^{-3}. Density initially increased fast, to 100 kg m^{-3} for 1-day-old snow. It reached approximately 200 kg m^{-3} for depth hoar. In November, due to frequent snowfalls, a wide range of densities was observed in the snowpack. Density then tended to homogenize in the lower layers because compaction was compensated by upward water vapor fluxes, producing mass loss. As observed earlier (*18*), the late season snowpack density in Fairbanks was fairly constant with height, in contrast to Arctic snowpacks, where wind-packed layers up to 520 kg m^{-3} in density alternate with much lighter depth hoar layers (*1*).

As SSA decreases with snow aging (*24*, *28*, *32*, *33*), it decreased with depth inside the snowpack. Freshly fallen snow SSA values ranged from about 800 $cm^2\ g^{-1}$ for bullet rosettes and columns to 1171 $cm^2\ g^{-1}$ for very rimed dendritic snow. A day after a snowfall, when crystals were still recognizable, SSA had generally decreased to half its initial value. SSA of well faceted crystals, regardless of their initial shape, was approximately 200 ± 50 $cm^2\ g^{-1}$ and dropped to 90 ± 20 $cm^2\ g^{-1}$ for depth hoar. In early winter, the snowpack SSA values showed a wide range (Figure 3a). Subsequently, with depth hoar growing at the base and with rarer snowfalls, SSA showed moderate values at the top, dropped in the first few centimeters, and leveled off to a value lower than 100 $cm^2\ g^{-1}$ (Figure 3d).

Snow Area Index. The SAI of the snowpack was deduced by summing the SAI of all snow layers (*1*)

$$\mathrm{SAI}_{\mathrm{snowpack}} = \sum_i \mathrm{SSA}_i h_i \rho_i \qquad (1)$$

with h being the height of layer i and ρ its density. Figure 4 shows the SAI evolution during winter. The accuracy is estimated at 16%. As the snowpack built up, the SAI increased,

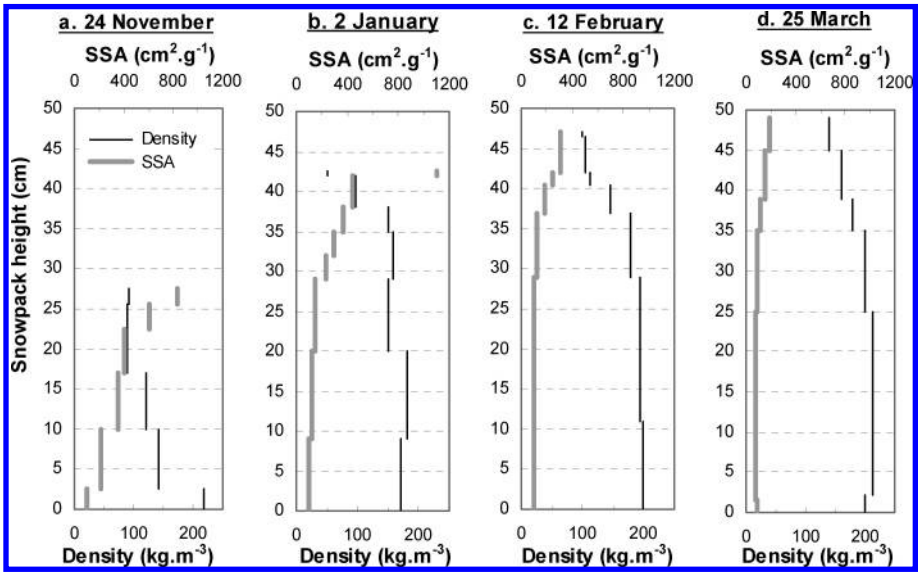

FIGURE 3. Density (kg m^{-3}) and SSA (cm^2 g^{-1}) profiles at four stages of the winter season.

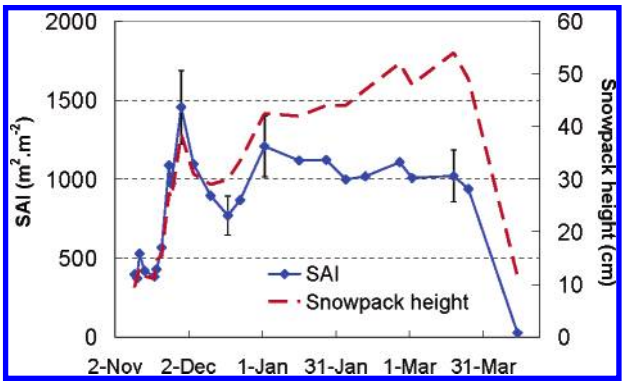

FIGURE 4. Evolution of the snow area index (SAI) and of snowpack height over the winter season. SAI values were 1088, 1208, 1019, and 938 m^2 m^{-2} on November 24, January 2, February 12, and March 25, respectively.

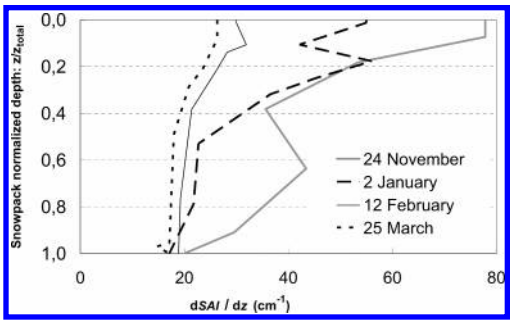

FIGURE 5. Vertical distribution of SAI as a function of normalized depth.

reaching 1460 m^2 m^{-2} at the end of November. Because of reduced precipitation in winter relative to fall and because of the decrease in SSA of each snow layer, the SAI actually dropped from its late fall maximum down to a value around 1000 at the end of winter.

Discussion

Vertical Distribution of the SAI. Surface snow layers are more likely to interact with the atmosphere than deeper layers. We therefore determined how the SAI was distributed vertically, using eq 2

$$\frac{\mathrm{d(SAI)}}{\mathrm{d}z} = \mathrm{SSA} \times \rho \qquad (2)$$

where z is the snowpack depth. Figure 5 shows the vertical distribution of SAI at four stages of winter. With 12% accuracy on SSA and 5% on density, the accuracy on d(SAI)/dz is 13%. In November, frequent precipitations produced a high SAI at the top of the snowpack. The rapid metamorphism driven by strong early season temperature gradients (Figure 1) caused fast SSA and SAI decreases with depth. On the contrary, in February and March, infrequent precipitation and the transformation of most of the snowpack to depth hoar resulted in a fairly homogeneous vertical distribution of SAI. Although Figure 4 shows that from January onward the snowpack SAI is almost constant, Figure 5 suggests that changes in its vertical distribution may in some cases affect the actual air−snow interaction potential. On timescales short enough so that only the top 5 cm of the snowpack are involved in air−snow exchanges, the accessible SAI decreased by a factor of 2.5 between November 24 and March 25.

The SAI of the subarctic snowpack can be compared to that of the Arctic snowpack at Alert (*1*) (Canadian Arctic, 82°30′ N). After correction of their values for CH_4 adsorption on stainless steel (*24*), we find that the Arctic snowpack SAI at Alert was 1595 m^2 m^{-2} on February 8, 2000, and 2525 m^2 m^{-2} on April 18, 2000, significantly greater than in the subarctic. This is mainly because most of the Arctic snowpack mass is formed by windpacked layers that have a higher SSA and a greater density than the depth hoar layers (*14*) predominant in the subarctic. The Arctic snowpack shows a lot of spatial variability. However, our observations around Alert and in Northern Alaska suggest that as a general rule, the presence of windpacks of large SAI guarantees that the Arctic SAI is almost always larger than the subarctic SAI. Confirming this statement, we measured a snowpack SAI near Barrow (Alaskan Arctic coast, 71° N) of 3330 on April 2, 2004 (*34*).

Implications for Atmospheric Composition and Climate Change. SVOCs in general and persistent organic pollutants (POPs) in particular are a subject of concern in environmental chemistry because of their environmental impact. As shown in recent measurements and models, snow is an efficient vector that transfers SVOCs from the atmosphere to northern and temperate terrestrial ecosystems (*3*, *35*, *36*). Recent work implicitly suggests that snow SSA and snowpack SAI are crucial variables that determine the efficiency of this vector (*10*, *15*), because these SVOCs sorb to snow surfaces. With the examples of 2,4,4′-trichlorobiphenyl (PCB 28) and of

TABLE 1. Calculated Distributions of 1 ng of PCB 28 and of PCB 180 in the System Formed by the March 25, 2004, Subarctic Snowpack of Figure 2 and a 400 m High Boundary Layer over a Surface Area of 1 m^2 [a]

	thickness (m)	mean temp (°C)	SAI (m^2 m^{-2})	PCB 28 concn (pg m^{-2})	PCB 28 % in layer	PCB 180 concn (pg m^{-2})	PCB 180 % in layer
atmospheric boundary layer	400	−16	-	713	71	61	6
surface layer	0.04	−17.3	105 (11%)	86	9	282	28
top faceted layer	0.06	−13.1	142 (15%)	64	6	208	21
bottom faceted layer	0.04	−10.2	84 (9%)	25	3	82	8
intermediate layer	0.1	−9.0	180 (19%)	45	5	148	15
depth hoar	0.25	−5.5	427 (46%)	67	7	219	22
		total snowpack		287	29	939	94

[a] The percentage of SAI contributed by each layer to the total snowpack SAI is indicated. The partitioning of both PCBs between the boundary layer and each snow layer is also given.

TABLE 2. Calculated Distributions of 1 ng of PCB 28 and of PCB 180 in the System Formed by the April 18, 2000, Arctic Snowpack at Alert (Domine et al., 2002) with a SAI of 2525 m^2 m^{-2} and a 400 m High Boundary Layer over a Surface Area of 1 m^2 [a]

	thickness (m)	mean temp (°C)	SAI (m^2 m^{-2})	PCB 28 concn (pg m^{-2})	PCB 28 % in layer	PCB 180 concn (pg m^{-2})	PCB 180 % in layer
atmospheric boundary layer	400	−26	-	61	6	2	0.2
recent surface layers	0.04	−27	120 (5%)	36	4	38	4
hard windpack	0.06	−29	890 (35%)	369	37	393	39
faceted crystals	0.04	−28.5	295 (12%)	113	11	120	12
hard windpack	0.1	−28	1000 (39.5%)	353	35	376	38
depth hoar	0.25	−27	220 (8.5%)	66	7	71	7
		total snowpack		939	94	998	99.8

[a] The percentage of SAI contributed by each layer to the total snowpack SAI is indicated. The partitioning of both PCBs between the boundary layer and each snow layer is also given.

2,2′,3,4,4′,5,5′-heptachlorobiphenyl (PCB 180), which are frequently measured in snow and air (*10*, *15*), we test the potential of the subarctic snowpack to take up SVOCs from the atmosphere. Using the data of Dominé et al. (*1*), we also perform calculations for the Arctic, where SAI is much greater. These two PCBs were selected as representative of a wide range of volatility: PCB 28 is fairly volatile, while PCB 180 is among the least volatile POPs. Their calculated vapor pressures over their liquid at 25 °C are respectively 0.027 and 0.00011 Pa (*37*).

The temperature dependence of the adsorption coefficient of PCB 28, $K_{SA}(T)$, was calculated using a van't Hoff equation and estimated values (*4*) of $K_{SA}(-6.8\ °C)$ and of the enthalpy of adsorption, ΔH_a,

$$\log K_{SA}(T) = \log K_{SA}(-6.8\ °C) + \frac{\Delta H_a}{2.303R}\left(\frac{1}{T} - \frac{1}{T_{-6.8°C}}\right) \quad (3)$$

where R is the ideal gas constant and T is the temperature in degrees kelvin. We consider a column with a 1 m^2 surface area, in which 1 ng of PCB 28 and 1 ng of PCB 180 partition between the snowpack and a 400 m thick boundary layer. Since we assume a linear relationship between PCB mixing ratios and the amounts adsorbed on snow, partitioning results do not depend on the amounts. Calculations are made for the March 25 conditions (Figures 2d and 3d). The air temperature is assumed to be constant throughout the boundary layer, and PCB concentrations in the snowpack are calculated discretely in the main layers, using temperature data from the vertical string of sensors. Table 1 indicates that the 25 March snowpack (SAI = 938) sequesters 28% of the PCB 28 available in the system composed of the boundary layer and the snowpack. This fraction increases to 94% for the less volatile PCB 180.

Similar calculations (Table 2) for the April 18, 2000, Arctic snowpack at Alert (82°30′ N) mentioned above show that the Arctic snowpack sequesters 94% of PCB 28 and almost all of PCB 180 (99.8%). This greater storage capacity is because the Arctic snowpack is colder and has a greater SAI due to the presence of windpacks. The Arctic snowpack therefore appears as more efficient in the uptake of SVOCs than the subarctic snowpack.

However, the subarctic snowpack may exchange chemicals with the atmosphere much more rapidly, for three reasons. First, it is much more permeable, as depth hoar is at least 10 times more permeable than windpacks (*38*). Second, active convection in the subarctic snowpack enhances exchanges (*39*). Third, ice layers of low permeability are less likely to last long in the subarctic snowpack, because the vigorous metamorphism rapidly transforms them into depth hoar of high permeability (*39*). Although such layers were not observed at Alert (82° N), they are often present at lower latitudes, such as Barrow (71° N).

During spring, the warming and melting of the snowpack leads to the emission of a fraction of adsorbed compounds to the atmosphere, the rest being transferred to ecosystems by runoff (*10*). Because of its increased reservoir capacity and its lower ability for exchange, we speculate that the Arctic snowpack will be much more efficient in the transfer of adsorbed species from the atmosphere to ecosystems. The

pulse of POPs modeled by Daly and Wania (*10*) may then be considerably attenuated in the subarctic. This illustrates the importance of considering the details of snowpack physics to quantify its chemical role.

Global warming will modify snowpack physical properties. For example, shrubs will grow on the tundra (*40*, *41*), shielding the snow from wind action. Less compacted and more permeable snow will then be more likely to evolve into depth hoar. This will reduce the reservoir capacity of the snowpack for adsorbed pollutants and enhance its ability to release them to the atmosphere before snowmelt. As high latitudes warm up, the ability of the tundra snowpack to transfer POPs and SVOCs from the Arctic atmosphere to high latitude ecosystems will then probably be reduced. From Tables 1 and 2, we suggest that this effect will be more pronounced for the more volatile SVOCs, while heavy compounds such as PCB 180 will be little affected, as they will still be taken up efficiently by warmer snowpacks of low SAI: 70% of the stored PCB 28 will be lost to the atmosphere if conditions change from Arctic to subarctic ones, while that fraction will only be 6% for PCB 180.

Acknowledgments

This work was partially supported by Chapman Chair funds, kindly supplied by Pr. Norbert Untersteiner. A.S.T. and F.D. thank the Geophysical Institute, University of Alaska Fairbanks, for hosting them during this work, while they were supported by CNRS and the French Ministry of Research. Additional funds were supplied by the International Arctic Research Center to partially support A.S.T. We gratefully thank Bill Hauer, for proposing the LARS site for this study and for assistance throughout the field work, and Hajo Eicken, for the use of the cold rooms. The term "snow area index" was suggested by Paul B. "SnowBlaster" Shepson.

Supporting Information Available

Photomicrographs of snow crystals of the subarctic snowpack at various stages of evolution. This material is available free of charge via the Internet at http://pubs.acs.org.

Literature Cited

(1) Dominé, F.; Cabanes, A.; Legagneux, L. Structure, microphysics, and surface area of the Arctic snowpack near Alert during the ALERT2000 campaign. *Atmos. Environ.* **2002**, *36*, 2753−2765.

(2) Dominé, F.; Shepson, P. B. Air-snow interactions and atmospheric chemistry. *Science* **2002**, *297*, 1506−1510.

(3) Franz, T. P.; Eisenreich, S. J. Snow scavenging of polychlorinated biphenyls and polycyclic aromatic hydrocarbons in Minnesota. *Environ. Sci. Technol.* **1998**, *24*, 1771−1778.

(4) Lei, Y. D.; Wania, F. Is rain or snow a more efficient scavenger of organic chemicals? *Atmos. Environ.* **2004**, *38*, 3557−3571.

(5) Hutterli, M. A.; Bales, R. C.; McConnell, J. R.; Stewart, R. W. HCHO in Antarctic snow: Preservation in ice cores and air-snow exchange. *Geophys. Res. Lett.* **2002**, *29*, 1235.

(6) Beine, H. J.; Honrath, R. E.; Dominé, F.; Simpson, W. R.; Fuentes, J. D. NOx during background and ozone depletion periods at Alert: Fluxes above the snow surface. *J. Geophys. Res.* **2002**, *D107*.

(7) Perrier, S.; Houdier, S.; Dominé, F.; Cabanes, A.; Legagneux, L.; Sumner, A. L.; Shepson, P. B. Formaldehyde in Arctic snow. Incorporation into ice particles and evolution in the snowpack. *Atmos. Environ.* **2002**, *36*, 2695−2705.

(8) Houdier, S.; Perrier, S.; Dominé, F.; Grannas, A. M.; Guimbaud, C.; Shepson, P. B.; Boudries, H.; Bottenheim, J. W. Acetaldehyde and acetone in the Arctic snowpack during the ALERT2000 field campaign. Snowpack composition, incorporation processes and atmospheric impact. *Atmos. Environ.* **2002**, *36*, 2609−2618.

(9) Dominé, F.; Lauzier, T.; Cabanes, A.; Legagneux, L.; Kuhs, W. F.; Techmer, K.; Heinrichs, T. Snow metamorphism as revealed by scanning electron microscopy. *Microsc. Res. Tech.* **2003**, *62*, 33−48.

(10) Daly, G. L.; Wania, F. Simulating the influence of snow on the fate of organic compounds. *Environ. Sci. Technol.* **2004**, *38*, 4176−4186.

(11) Macdonald, R. W.; Harner, T.; Fyfe, J. Recent climate change in the Arctic and its impact on contaminant pathways and interpretation of temporal trend data. *Sci. Total Environ.* **2005**, *342*, 5−86.

(12) Villa, S.; Vighi, M.; Maggi, V.; Finizio, A.; Bolzacchini, E. Historical trends of organochlorine pesticides in an alpine glacier. *J. Atmos. Chem.* **2003**, *46*, 295−311.

(13) Legrand, M.; Mayewski, P. Glaciochemistry of polar ice cores: A review. *Rev. Geophys.* **1997**, *35*, 219−243.

(14) Legagneux, L.; Cabanes, A.; Dominé, F. Measurement of the specific surface area of 176 snow samples using methane adsorption at 77 K. *J. Geophys. Res.* **2002**, *107*, 4335.

(15) Herbert, B. M. J.; Halsall, C. J.; Villa, S.; Jones, K. C.; Kallenborn, R. Rapid changes in PCB an OC pesticide concentrations in Arctic snow. *Environ. Sci. Technol.* **2005**, *39*, 2998−3005.

(16) Bremond, L.; Alexandre, A.; Hély, C.; Guiot, J. A phytolith index as a proxy for tree cover density in tropical areas: Calibration with leaf area index along a forest−savanna transect in southeastern Cameroon. *Global Planet. Change* **2005**, *45*, 277−293.

(17) Sturm, M.; Holmgren, J.; Liston, G. E. A seasonal snow cover classification system for local to global applications. *J. Climate* **1995**, *8*, 1261−1283.

(18) Sturm, M.; Benson, C. S. Vapor transport, grain growth and depth hoar development in the subarctic snow. *J. Glaciol.* **1997**, *43*, 42−59.

(19) Hanot, L.; Dominé, F. Evolution of the surface area of a snow layer. *Environ. Sci. Technol.* **1999**, *33*, 4250−4255.

(20) Dominé, F.; Taillandier, A.-S.; Simpson, W. R.; Severin, K. Specific surface area, density and microstructure of frost flowers. *Geophys. Res. Lett.* **2005**, *32*, L13502.

(21) Akitaya, E. Studies on depth hoar. Contributions from the Institute of Low Temperature Science **1974**, *26* (Series A), 1−67.

(22) Marbouty, D. An experimental study of temperature-gradient metamorphism. *J. Glaciol.* **1980**, *26*, 303−312.

(23) Brunauer, S.; Emmet, P. H.; Teller, E. Adsorption of gases in multimolecular layers. *J. Am. Chem. Soc.* **1938**, *60*, 309−319.

(24) Legagneux, L.; Taillandier, A.-S.; Dominé, F. Grain growth theories and the isothermal evolution of the specific surface area of snow. *J. Appl. Phys.* **2004**, *95*, 6175−6184.

(25) Dominé, F.; Taillandier, A.-S.; Simpson, W. R. A parameterization of the specific surface area of snow in models of snowpack evolution, based on 345 measurements. *J. Geophys. Res.* submitted.

(26) Hedstrom, N. R.; Pomeroy, J. W. Measurements and modelling of snow interception in the boreal forest. *Hydrol. Process.* **1998**, *12*, 1611−1625.

(27) Sturm, M.; Benson, C. S. Scales of spatial heterogeneity for perennial and seasonal snow layers. *Ann. Glaciol.* **2004**, *38*, 253−260.

(28) Legagneux, L.; Lauzier, T.; Dominé, F.; Kuhs, W. F.; Heinrichs, T.; Techmer, K. Rate of decay of the specific surface area of snow during isothermal experiments and morphological changes studied by scanning electron microscopy. *Can. J. Phys.* **2003**, *81*, 459−468.

(29) Colbeck, S. C.; Akitaya, E.; Armstrong, R.; Gubler, H.; Lafeuille, J.; Lied, K.; McClung, D.; Morris, E. *The international classification for seasonal snow on the ground*. Wallingford, Oxfordshire, International Association of Scientific Hydrology. International Commission of Snow and Ice, 1990.

(30) Dominé, F.; Cabanes, A.; Taillandier, A.-S.; Legagneux, L. Specific surface area of snow samples determined by CH_4 adsorption at 77 K and estimated by optical microscopy and scanning electron microscopy. *Environ. Sci. Technol.* **2001**, *35*, 771−780.

(31) Taillandier, A.-S.; Domine, F.; Simpson, W. R.; Sturm, M.; Douglas, T. A. The rate of decrease of the specific surface area of dry snow: isothermal and temperature gradient conditions *J. Geophys. Res.*, submitted.

(32) Cabanes, A.; Legagneux, L.; Dominé, F. Evolution of the specific surface area and of crystal morphology of Arctic fresh snow during the ALERT2000 campaign. *Atmos. Environ.* **2002**, *36*, 2767−2777.

(33) Cabanes, A.; Legagneux, L.; Dominé, F. Rate of evolution of the specific surface area of surface snow layers. *Environ. Sci. Technol.* **2003**, *37*, 661−666.

(34) Taillandier, A.-S.; Domine, F., unpublished results.

(35) Hung, H.; Blanchard, P.; Halsall, C. J.; Bidleman, T. F.; Stern, G. A.; Fellin, P.; Muir, D. C. G.; Barrie, L. A.; Jantunen, L. M.; Helm, P. A.; Ma, J.; Konoplev, A. Temporal and spatial variabilities of

atmospheric polychlorinated biphenyls (PCBs), organochlorine (OC) pesticides and polycyclic aromatic hydrocarbons (PAHs) in the Canadian Arctic: Results from a decade of monitoring. *Sci. Total Environ.* **2005**, *342*, 119−144.

(36) Gustafsson, Ö.; Andersson, P.; Axelman, J.; Bucheli, T. D.; Kömp, P.; McLachlan, M. S.; Sobek, A.; Thörngren, J.-O. Observations of the PCB distribution within and in-between ice, snow, ice-rafted debris, ice-interstitial water, and seawater in the Barents Sea marginal ice zone and the North Pole area. *Sci. Total Environ.* **2005**, *342*, 261−279.

(37) Li, N.; Wania, F.; Lei, Y. D.; Daly, G. L. A comprehensive and critical compilation, evaluation, and selection of physical−chemical property data for selected polychlorinated biphenyls. *J. Phys. Chem. Ref. Data* **2003**, *32*, 1545−1590.

(38) Albert, M. R.; Shultz, E. F. Snow and firn properties and air−snow transport processes at Summit, Greenland. *Atmos. Environ.* **2002**, *36*, 2789−2797.

(39) Sturm, M.; Johnson, J. Natural convection in the subarctic snow cover. *J. Geophys. Res.* **1991**, *96*, 11657−11671.

(40) Sturm, M.; McFadden, J. P.; Liston, G. E.; Chapin, F. S., III; Racine, C. H.; Holmgren, J. Snow−shrub interactions in Arctic tundra: A hypothesis with climate implications. *J. Climate* **2001**, *14*, 336−344.

(41) Sturm, M.; Racine, C. H.; Tape, K. Increasing shrub abundance in the Arctic. *Nature* **2001**, *411*, 546−547.

Received for review April 7, 2006. Revised manuscript received September 26, 2006. Accepted October 5, 2006.

ES060842J